

Design and development of biogas electrical power generation with an adaptive control mechanism for rural electrification

Vineeth Kumar Pothera Kariyat, Jijesh Jisha Janardhanan

Department of Electronics and Communication Engineering, Sri Venkateshwara College of Engineering,
Visvesvaraya Technological University, Bangalore, India

Article Info

Article history:

Received Nov 16, 2022

Revised Apr 11, 2023

Accepted Apr 24, 2023

Keywords:

Adaptive control mechanism

Biogas power generation

Biogas reactor

PMDC motor

PMSG

ABSTRACT

The primary goal of this research is to implement a model of biogas power generation unit used for rural electrification. A biogas reactor, a microturbine, a permanent magnet synchronous generator (PMSG), a rectifier, and a permanent magnet DC motor (PMDC) make up the proposed system. The biomass used to fuel the biogas reactor is typically derived from the surplus agricultural and animal waste found in rural areas. The operation of the biogas power system, design, and detailed mathematical modeling of each segment is described in this paper. In addition to that, an adaptive control mechanism is added to improve the system stability. The MATLAB/Simulink environment is used to develop the overall biogas fueled power system and thus obtained various parameters. The observation in the development has shown an improvement in biogas power generation unit's suitability for standalone applications such as water pumping in rural area.

This is an open access article under the [CC BY-SA](https://creativecommons.org/licenses/by-sa/4.0/) license.



Corresponding Author:

Vineeth Kumar Pothera Kariyat

Department of Electronics and Communication Engineering, Sri Venkateshwara College of Engineering

Visvesvaraya Technological University

Bangalore, India

Email: vineethkumarpk@gmail.com

1. INTRODUCTION

Renewable energy sources such as biomass are becoming increasingly important to address the rising energy demand. Solar energy is used to create biomass, which has a strong potential to replace fossil fuels. It includes the main advantage of biomass over other renewable energy sources (RES) is the easiness of storage. It can deliver a constant and non fluctuating supply of electricity and heat. Biomass is burned to produce heat and electricity or biofuel. The energy from biomass is extracted using fuel combustion, gasification, digestion, and fermentation. In this research work, the biogas extracted from biomass using the fuel combustion process is considered. Converting biomass to electrical energy can be done in different ways. The major challenges of the biogas fuel-powered system are discussed here. Anaerobic digestion (AD) is one of the popular methods to extract biogas from biomass. AD takes place without the presence of oxygen. But the implementation of the AD process is quite complex due to the following reasons: variation of input variable leads to damage to bacterial life, AD process [1], is non-linear, compound, and high dimensional. The performance of a biogas reactor depends on the volume of the reactor, type of biomass used, and moisture content. In this regard, biogas fuel-powered systems must be adjusted to assure safety, increase efficiency, and reduce costs. The main functions of control algorithms are: to regulate the produced methane flow with respect to load and keep the volatile fatty acid concentration at a safe limit.

There are different methods to simulate and model biogas fuel power systems. Biogas fuel power system consists of biogas reactor, microturbine, permanent magnet synchronous generator (PMSG) 3- ϕ

uncontrolled rectifier, and DC pump. Hill’s model describes detailed modeling of biogas reactor and analysis of methane gas production with respect to time. It is observed that analysis of only the dairy manure-based biogas power generation system [2], is explained in hill’s model. Fawzy *et al.* [3], described the steady-state and dynamic model of the AD process and estimated the importance of pH value during the AD process. Kasinath *et al.* [4], presented the four processes involved in biogas reactor and estimated the relation of each process. Hampel and Braun [5], Achinas *et al.* [6] used a genetic algorithm optimization model to find the relationship between methane gas output and electrical power output in a biogas fuel power system. In this analysis as the methane output increases from the biogas reactor the power output of the system increases. Kim *et al.* [7], describes model predictive control (MPC) which is used as the best control of the AD process in a biogas reactor. By using the state space model the MPC algorithm is developed. MPC helps in detecting the control inputs which results in system behavior prediction based on load change. The microturbine has the following advantages: less number of moving parts, lightweight, greater efficiency, and ability to utilize waste fuel [8]. Oppong *et al.* [9], describe mathematical equations for the modeling of microturbine. The control parameters are fuel temperature, speed of the turbine, acceleration fuel flow, and torque. PMSG is one of the best choices for biogas fuel power systems due to the following reasons: no requirement of external excitation, reduced conductor losses, high reliability, and efficiency [10]. The mathematical modeling of the PMSG is described in the research paper [11]. A permanent magnet synchronous generator, microturbine with adaptive control, power diode rectifier, and permanent magnet dc motor are all included in the proposed system as independent models. Each model in this system is integrated, and the energy flow is verified. Depending upon the application, each model can be used individually or in combination. Hence, the proposed system is appropriate for rural areas where the traditional grid is not practical.

The main contents of this manuscript briefly discuss upon: i) the mathematical model of biogas reactor, microturbine, PMSG, three phase uncontrolled rectifier, and DC pump, and ii) the adaptive control of biogas fuel power system. The section 2 covers system details; section 3 explains the modeling of the biogas fuel power system. The section 4 discusses simulation results. The last section concludes the research work.

2. RESEARCH METHOD

The biogas fuel power system consists of biogas reactor, microturbine, PMSG, three phase rectifier, and DC pump [12]. The schematic representation of the biogas power generation unit is shown in Figure 1. It can be observed that Figure 1(a) represents the general block diagram of biogas power generation, and Figure 1(b) represents the steps involved in the AD process of the biogas reactor. Each stage of the AD process is briefly described here.

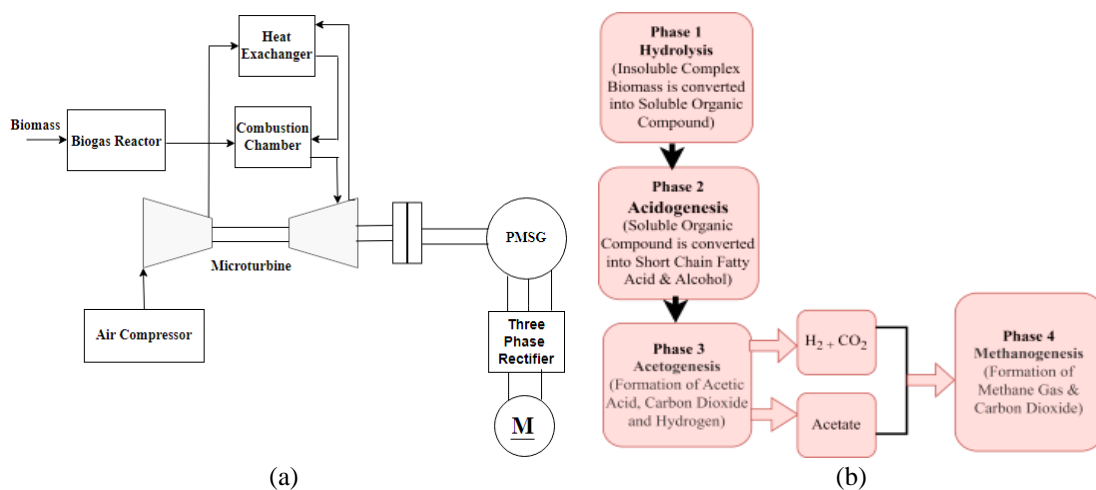


Figure 1. The biogas power generation; (a) general block diagram and (b) AD process in biogas reactor

The biogas reactor is a part of biogas fuel power system which converts biomass such as dairy manure into biogas in the absence of oxygen. The biogas output is given to the combustion chamber, and combustion occurs. The air compressor produces high pressurized air, which helps to increase the temperature of the combustion chamber. Thereby high-pressure steam is produced, which is capable of operating the microturbine. The excess heat produced in microturbine is reutilized using a heat exchanger and supplied back

to the combustion chamber to improve fuel combustion efficiency. It improves the overall efficiency of the microturbine. The processes involved in the biogas reactor are briefly described here.

2.1. Hydrolysis

Hydrolysis is the first step of AD. AD is the process that takes place without the presence of oxygen. In hydrolysis process, insoluble complex biomass is converted into the soluble organic compound in the presence of hydrolytic bacteria, proteins, lipids, and carbohydrates are all transformed into sugars, ammonia acids, and fatty acids in this process.

2.2. Acidogenesis

The process of converting soluble organic compounds to short chain fatty acid and alcohol is known as acidogenesis process. Acidogenesis is the second stage of the anaerobic digestion process also known as fermentation process. The bacteria involved in this process are known as acid formers. The water and acetic acid (CH_3COOH) are transformed into hydrogen (H_2) and carbon dioxide (CO_2) at the end of this process.

2.3. Acetogenesis

Acetogenesis is the third stage of the AD process. Carbon dioxide, acetic acid and hydrogen are formed from short-chain fatty acid and alcohol is known as acetogenesis. It involves the hydrogenation and dehydrogenation process.

2.4. Methanogenesis

Methanogenesis is considered the last phase of the AD process. The end product of methanogenesis is methane gas (CH_4), carbon dioxide (CO_2), and water (H_2O). The methanogenesis process has two stages. In the first stage, acetic acid is converted into methane, and in the second stage, hydrogen is converted into methane by utilizing carbon dioxide. The overall anaerobic digestion process in the biogas reactor is shown in the Figure 1(b). Dairy manure is fed into the biogas digester. Biogas is produced after the retention period. In general retention period for dairy, manure is around 45 days. The fixed dome type biogas reactor is generally used for power generation. In fact, the methane gas output depends on the temperature of the reactor (T_{react}), the reactor volume (V), summation of volatile fatty acids concentration in reactor (S_v), methanogens concentration (X_{meth}), and constant monod half velocity for methanogens (K_{sc}). Amount of methane gas from the biogas reactor is given in the (1).

$$F_{\text{meth}} = V \left[\frac{(0.013T_{\text{react}} - 0.129)}{\left(\frac{K_{sc}}{S_v} + 1\right)} \right] K_4 X_{\text{meth}} \quad (1)$$

Let the volume of the reactor (V) is 20 m^3 , reactor temperature (T_{react}) is $950 \text{ }^\circ\text{C}$, net volatile fatty acids concentration in reactor (S_v) is 85, methogens concentration (X_{meth}) is 0.35 kg/m^3 and constant monod half velocity for metanogens (K_{sc}) is 21.5. To calculate the amount of methane gas output a constant (c) 35.4 is taken into consideration. The ratio of F_{meth} and constant (c) gives the total amount of biogas generated. Therefore by substituting above mentioned parameters in the (1), the total amount of biogas is 6.33 m^3 . The concentration of various biomass are shown in Table 1.

Table 1. Concentration of different biomass

Sl. No	Types of biomass	Concentration (kgm^{-3})
1	Dairy maure	0.36
2	Poultry	0.7
3	Beef	0.65
4	Swine	0.9

The concentration is directly proportional to the volume of methane output. It is observed that swine feed has the highest concentration, and it takes less period to produce constant methane output. In the case of dairy manure and beef feed, it takes a more extended period to deliver constant methane.

2.5. Modeling of microturbine with adaptive control

Microturbines are smaller gas combustion turbines with a high-speed range and a power rating of 25-500 kW. It operates based on the brayton cycle in thermodynamics. Microturbines are relatively vibration-free and have low noise thereby it is easy to handle. Various fuels such as biodiesel, kerosene, natural gas and biogas are used. Microturbines' (MT's) adaptive control mechanism [13], includes compressor-turbine model, acceleration control, fuel flow control, temperature control, and governor speed control.

2.5.1. Speed control of microturbine

The MT’s primary control mode under partial load conditions is speed control. It estimates the speed-accuracy by calculating difference between reference speed (1 PU) and rotor speed of synchronous generator. The lag-lead compensator’s transfer function is used to model speed control. Output of a droop governor is in proportional to the speed error. Speed error signal is given to the input of the controller. The error signal is proportional to the rate of change in the controller’s output. Any increase in load causes a speed reduction, which will affect the system’s stability. Here, the adaptive control plays a major role. Figure 2 illustrates the microturbine’s adaptive control mechanism, which makes the system stable regardless of sudden load variation. The block diagram of turbine speed control is as described in Figure 2(a). Here, K is the controller gain, T₁ is the constant governor lead time, T₂ is the constant governor lag time, and Z is the constant that represents governor mode. In this speed controller, the values of parameters are T₁=0.4, T₂=1, Z=3, and K=25 respectively.

2.5.2. Temperature control of microturbine

The temperature controller at a predetermined firing temperature maintains the output power of the gas turbine, irrespective of atmospheric temperature and biogas fuel properties. When biogas is burned in a combustion chamber, heated exhaust gases are produced. The exhaust gases temperature is calculated by a thermocouple’s series embedded in radiation shields. The thermocouple output gives the actual temperature value in the microturbine, which is compared with the reference value of microturbine temperature. If the difference between actual and reference temperature is positive, the output of the temperature controller will obtain a high value. Conversely, if the actual and reference temperature difference is negative, the temperature controller’s output will receive the least value. When the signal is more depressed than the output of a speed controller, the previous value will drop through the least value gate (LVG), restricting the turbine’s power. The exhaust temperature is given as the input temperature to the temperature controller and the temperature control signals output is given to LVG. Temperature is another important parameter for the adaptive control mechanism illustrated in Figure 2. The temperature controller integration is T_t, time constants linked with the radiation shield are T₃ and thermocouple T₄, respectively, and the radiation shield constants K₁, K₂, and time constant of temperature controller T₅ [14], as shown in Figure 2(b). The values of parameters in the temperature controller are as follows: T₃=15, T₄=2.5, T₅=3.3, K₁=0.8, and K₂=0.2.

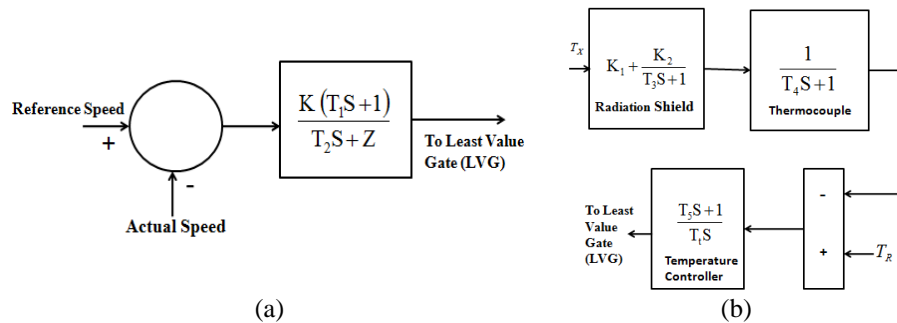


Figure 2. Adaptive control mechanism; (a) speed control and (b) temperature control

2.5.3. Acceleration control of microturbine

The acceleration control is used to find out the acceleration of the rotor before microturbine comes to its rated speed. The input signals for an LVG are generated by these control functions. There are three inputs to LVG: speed, acceleration, and temperature. The smallest among three inputs is provided to the fuel compressor turbine unit. Figure 3 depicts the adaptive control mechanism by considering acceleration and fuel system. Figure 3(a) illustrates the block diagram for acceleration control.

2.5.4. Fuel system control

The significant components of fuel system control are the actuator and fuel valve. From the fuel system actuator, the fuel is supplied through the valve positioner. The transfer function of fuel valve positioner’s is stated in (2).

$$E_1 = \left(\frac{K_v}{T_v S + C} \right) F_d \tag{2}$$

Where, E_1 is the output of valve positioner, K_v is the gain of valve positioner, T_v is the time constant of valve positioner, F_d is the input of valve positioner, and C is the constant for transfer function. The values of K_v , T_v , and C are 0.05, 1, and 1 respectively. The transfer function of fuel system actuator is given in (3).

$$W_f = \left(\frac{K_f}{T_f s + c} \right) E_1 \tag{3}$$

Where, W_f denotes fuel demand signal per unit, K_f represents fuel system actuator gain, T_f indicates fuel system actuator time constant, and E_1 is the output of valve positioner. The values of K_f , T_f are 1 and 0.04 respectively. The output of the least value gate is the minimum required fuel at a given operating point V_{ce} this output is provided into the fuel system. The second input to the fuel control system is speed of turbine (N) shown in Figure 3(b). V_{ce} 's per unit value is proportional to the per unit value of mechanical power on the turbine at stable conditions. Operating point is V_{ce} , as well as the lowest amount of fuel flow at no load is K_3 .

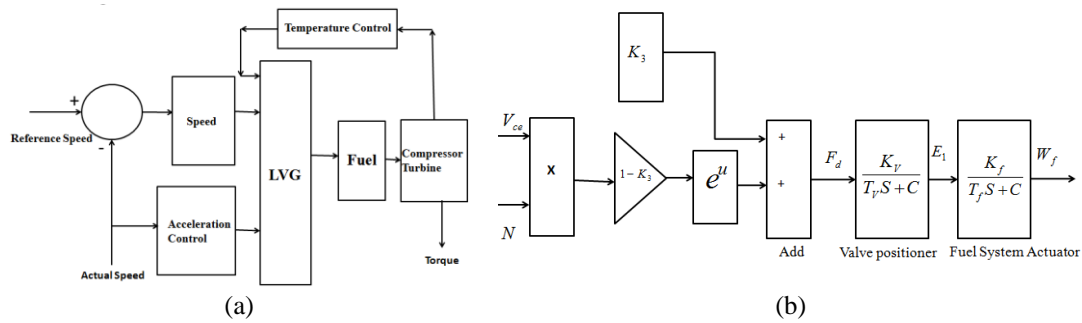


Figure 3. Adaptive control mechanism; (a) acceleration control and (b) fuel system control

2.5.5. Compressor-turbine model

The compressor helps to increase the gas pressure by reducing its volume. Here it supplies sufficient air to the combustion chamber and thereby combustion, takes place. At the end of this process, biogas is produced. The compressor turbine model block diagram is given in Figure 4.

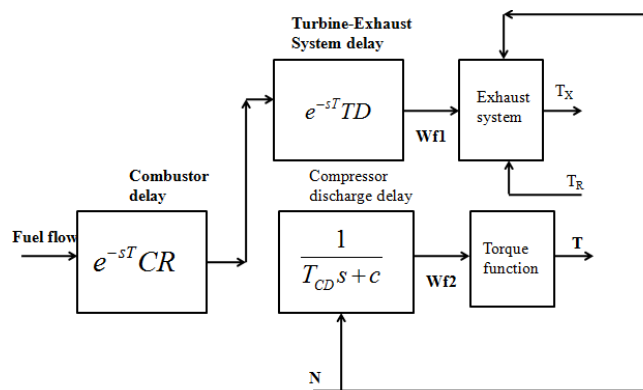


Figure 4. Compressor turbine model

Mechanical torque developed from the turbine is as discussed in (4):

$$T = K_H(W_f - 0.23) + 0.5(1 - N) \tag{4}$$

temperature of the turbine is given by the mathematical expression (5).

$$T_x = T_R - 700(1 - W_f) + 550(1 - N) \tag{5}$$

In (4) and (5), K_H is the coefficient depends on enthalpy, N denotes the speed of turbine, W_f indicates fuel, and T_R represents reference temperature. The complete MATLAB/Simulink model of microturbine is shown in Figure 5. There are five important mechanical parameters considered in adaptive control mechanism.

The adaptive control mechanism integrates governor speed control, fuel control system, acceleration control, temperature control system, and compressor turbine system. The output torque obtained from the microturbine is the function of speed, acceleration, fuel flow, and the temperature of the microturbine. It is observed that Figure 5 shows the integration of governor speed control, fuel control system, acceleration control, temperature control system and compressor turbine system.

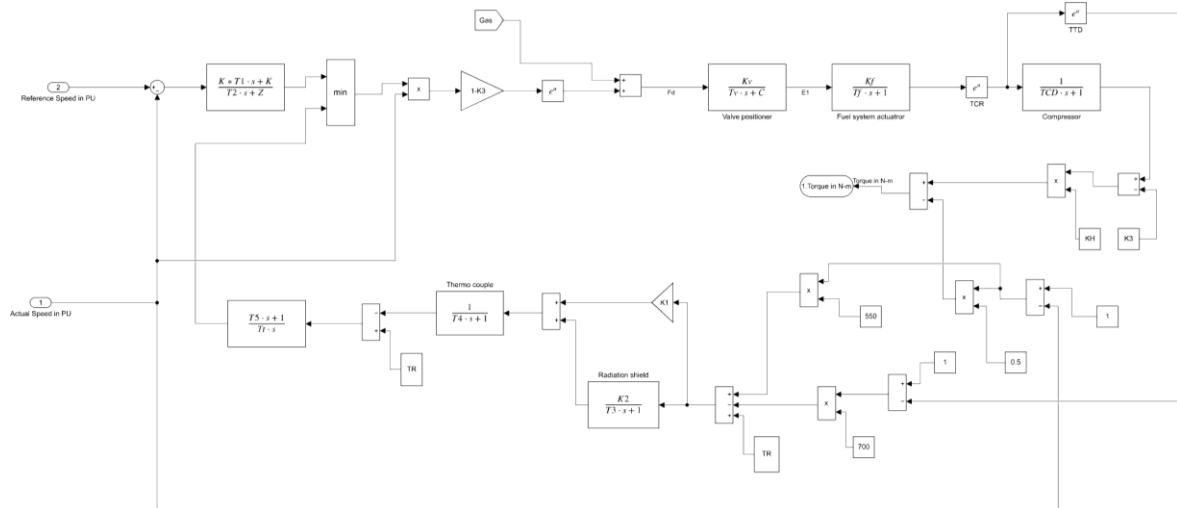


Figure 5. Simulink model of microturbine system

2.6. Modelling of permanent magnet synchronous generator

The microturbine is coupled with a four-pole high-speed PMSG with a non-salient rotor type to generate AC power in this research work. The generators’ electrical and mechanical components are represented using a second-order state-space modeling approach [15]. The stator flux is intended to be sinusoidal. The rotor of PMSG is made up of a permanent magnet, and the stator is made up of silicon steel. The stator is connected to the load. The stator’s 3- ϕ sinusoidal winding produces a synchronously revolving air gap flux. When a micro turbine [16], [17], rotates the PMSG, the stator windings produce balanced three-phase sinusoidal voltages. In case of PMSG, the dynamic model is produced from the two-phase synchronous reference frame, in which the direct axis is lagging 900 with the quadrature axis for the direction of rotation. To synchronize direct and quadrature axis rotating frame phase-locked loop (PLL) is used. The PMSG configuration [18], can be expressed using (6) and (7), respectively.

$$\frac{d}{dt} i_d = \frac{1}{L_d} V_d - \frac{R}{L_d} i_d + \frac{L_q}{L_d} P \omega_r i_q \tag{6}$$

$$\frac{d}{dt} i_q = \frac{1}{L_q} V_q - \frac{R}{L_q} i_q - \frac{L_d}{L_q} P \omega_r i_d - \frac{P \omega_r}{L_q} \tag{7}$$

The following assumptions were made for the operation of PMSG: i) stator windings are considered symmetrical, ii) damper windings are not considered, and iii) capacitive effect is neglected. By neglecting core losses, d-q axis voltage are written in (8) and (9), respectively:

$$V_d = R i_d + L \frac{d}{dt} i_d - \omega_r L i_q \tag{8}$$

$$V_q = R i_q + L \frac{d}{dt} i_q + \omega_r L i_d + \omega_r \tag{9}$$

the (10) describes the electromagnetic torque developed in the machine air gap.

$$T_e = \frac{3}{2} P (i_q + (L_d - L_q) i_d i_q) \tag{10}$$

Where the quadrature-axis voltage is V_q , the direct-axis voltage is V_d , the direct-axis current is i_d , the quadrature-axis current is i_q , the quadrature-axis inductance is L_q (165 μ H), the direct-axis inductance is L_d (165 μ H), the stator winding resistance is R (12.5 Ω), the angular speed of rotor is ω_r (70,000 rpm) and the number of poles is P (4 numbers). The main objective of this work is to develop the rural electrification system. The application selected for this work is DC water pumping. Therefore, the output of PMSG is connected to three phase diode rectifiers. The AC power to DC power is converted using three-phase uncontrolled diode rectifier. The output of the diode rectifier is given to the DC pumping unit.

2.6.1. Three phase uncontrolled diode rectifier

A three-phase uncontrolled diode rectifier is a power electronic circuit that converts three-phase AC power into DC power. The output of PMSG is connected to three-phase rectifiers, and rectified output is supplied to the PMDC motor. The mathematical model of the DC segment of the biogas-fueled power system is shown in Figure 6. The mathematical model of the DC segment of the biogas-fueled power system is shown in Figure 6. PMSG output is rectified and supplied to the PMDC, shown in Figure 6(a).

The diode rectifier is operated in continuous conduction mode. The diodes D_1 , D_3 and D_5 is categorized into a positive group whereas the diodes D_4 , D_6 and D_2 are considered as negative group. In this regard, at least one diode from each group must operate. The three- phase rectifier operates in six different conduction modes and each diode conducts at 120° . The operating sequences of diodes are D_1D_2 , D_2D_3 , D_3D_4 , D_4D_5 , D_5D_6 and D_6D_1 . Hence a constant DC voltage appears across PMDC motor. The main advantage of a three-phase uncontrolled diode rectifier is reduced ripple content at the output. Therefore, no additional filter is needed for the system [18].

2.6.2. Permanent magnet dc motor (PMDC)

DC motors are used where the load requires high starting torque and a wide speed range. A “PMDC” is a DC motor type that uses a permanent magnet to generate the magnetic field required for DC motor operation [19], [20]. Field control of this DC motor type is impossible because a permanent magnet’s magnetic field strength is fixed and cannot be changed externally. The rating of PMDC used in this work is 187 W, 24 V. In the mathematical modelling of the DC segment of biogas fueled power system shown in Figure 6, Figure 6(b) represents the equivalent circuit of PMDC. The following parameters are considered from the equivalent circuit: V_a is the input to PMDC, R_a and I_a are the armature resistance and current respectively, L_a is the inductance of armature winding and E_b is the self induced emf. Let J is the motor’s moment of inertia (kgm^2), ω is the angular speed of the motor in rad/sec, B is the coefficient of viscous friction (Nm-s/rad), k_b is the constant back emf, and k_t is the constant torque. The mathematical equations corresponding to electrical segments are written using KVL:

$$V_a = R_a I_a + L_a \frac{di_a}{dt} + E_b \quad (11)$$

$$E_b = K_b \omega \quad (12)$$

the using newton’s second law, mathematical related to mechanical segments are given in (13) and (14).

$$T_e = J \frac{d\omega}{dt} + B\omega + T_L \quad (13)$$

$$T_e = K_t I_a \quad (14)$$

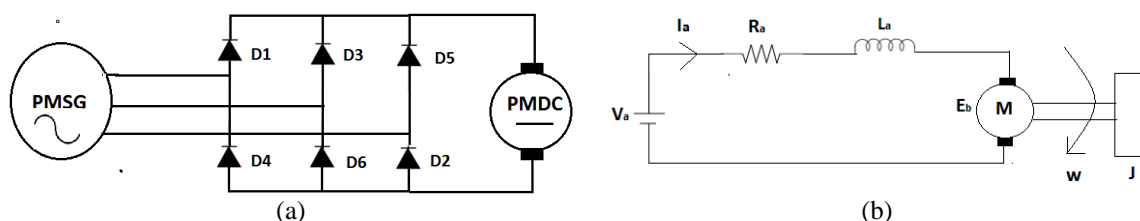


Figure 6. Mathematical model; (a) three phase diode rectifier and (b) PMDC motor

3. RESULTS AND DISCUSSION

The MATLAB/Simulink model [21] of the biogas fuel power system is illustrated in Figure 7. Biogas power generation system consists of biogas reactor, microturbine, PMSG, a three-phase rectifier supplied with a PMDC motor [22]–[25]. Figure 7 represents the complete model of biogas fueled power generation system that provides power to the DC water pump. The process of methanogenesis generates methane gas. The inputs to the microturbine are actual speed and the reference speed per unit to get torque as output. The output of the microturbine is coupled with PMSG. The output of PMSG is supplied to a step-down transformer. Later on, the output of step down transformer is connected to the three-phase uncontrolled rectifier, which is used to provide the PMDC motor.

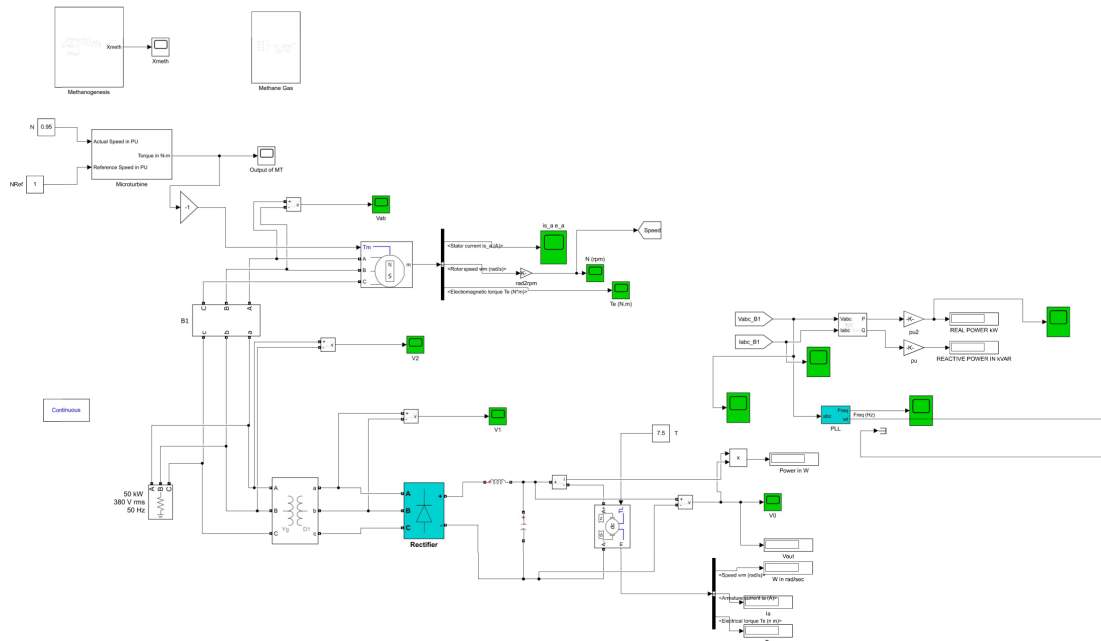


Figure 7. Simulink model of biogas fuel power system

Biogas power generation system parameters such as rotor speed, electromagnetic torque, frequency of power generation, the power delivered to the resistive load, output current, and output voltage of PMSG are plotted using MATLAB/Simulink software. The waveforms of biogas power generation system parameters are shown in Figures 8-11 respectively. Figure 8(a) shows the relation of rotor speed of PMSG versus simulation time. In this graph, the rotor speed becomes 70,000 rpm at 2 seconds. The rotor speed is steady after 1.5 s. As the load increases, the speed of the microturbine comes down slightly. However, the adaptive control system maintains the system stable irrespective of sudden changes in the load. Whenever the load increases, the torque of the microturbine is also increasing. Figure 8(b) shows electromagnetic torque produced by the microturbine. The magnitude of electromagnetic torque is estimated as -650 N-m. The electrical characteristics, such as frequency of power generation and power available across the load, illustrated in Figure 9. The frequency of generated voltage is given in Figure 9(a). It is observed that torque is steady once the methane reaches a constant volume. The model responds effectively when the torque changes in response to changes in load.

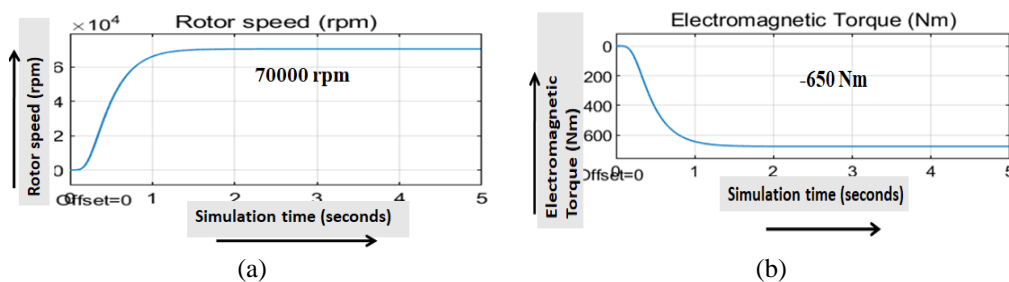


Figure 8. Mechanical characteristics; (a) rotor speed and (b) electromagnetic torque

It is obtained that the frequency of generated voltage is within the limit. The permissible grid frequency tolerance is $\pm 3\%$. The total amount of power delivered to the load is given in Figure 9(b). The magnitude of the power delivered to the load is 260 kW.

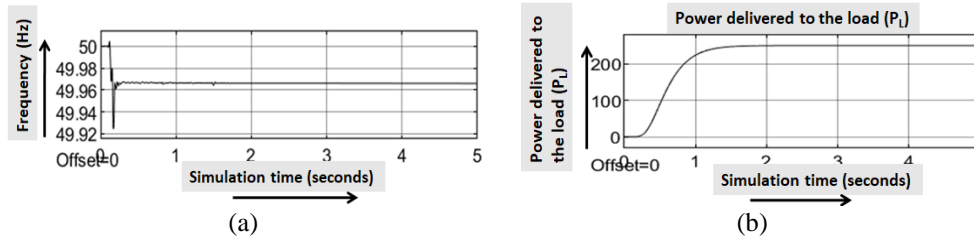


Figure 9. Electrical characteristics; (a) frequency of generated voltage in PMSG and (b) load power

The obtained value of line voltage is 1 PU. The voltage becomes steady at 1s, as indicated in Figure 10(a). The obtained value of current is displayed in Figure 10(b). The value of current passing through the load is 2.2 PU and becomes steady after 1.1s.

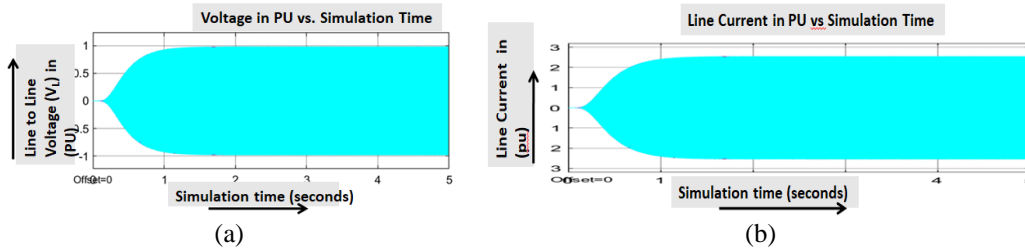


Figure 10. Electrical characteristics; (a) line voltage in PMSG and (b) line current in PMSG

The rating PMDC motor selected for this application is 187 W, 24 V. The terminal voltage obtained across the motor is 24 V. The terminal voltage of the DC motor is stable at 1.5 s, as shown in Figure 11(a). The graph of methane gas production to the number of days is given in Figure 11(b). The amount of methane gas production in the dairy manure-based biogas reactor for the retention period is plotted in Figure 11(b). Here the amount of methane output is expressed per unit value, and the retention period is expressed in terms of the number of days. It is observed that the methane gas production is stable after 20 days of the retention period. The amount of methane out varies depending on the type of biomass used. Table 1 provides the information on the concentration of biodegradable contents in various biomass inputs. The methane out depends on the amount of biodegradable concentration in the biomass. The detail of experimental validation is described here.

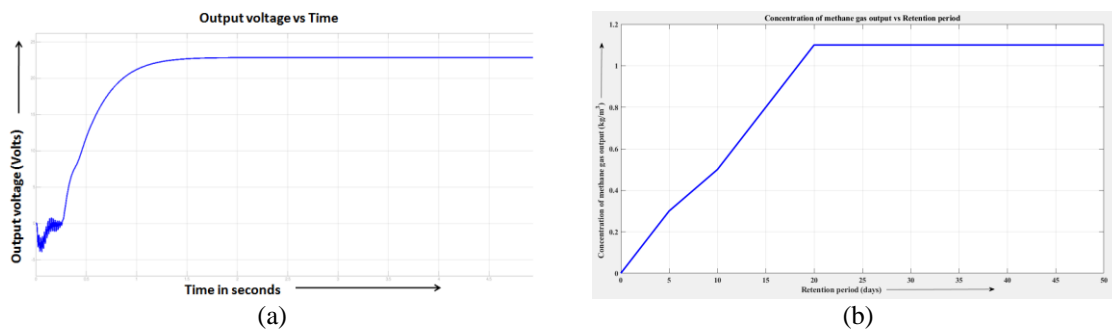


Figure 11. Parameters of biogas power generation; (a) output voltage of PMDC motor and (b) retention period

The experimental validation of the real-time biogas power generation system is being examined at the Siddhavana Gurukula in the Mangalore district of Karnataka; India is illustrated in Figure 12. In the system, a fixed dome type biogas reactor is employed. This biogas reactor's biomass input is cow dung. The reactor has a 20 m³ volume, and the biogas reactor typically produces 6.33 m³ of methane. Reactor temperature in this plant is kept at up to 950 °C, and retention times vary from 25 to 45 days.



Figure 12. Experimental validation of biogas power generation

4. CONCLUSION

This research work explains the mathematical modeling of the biogas fuel power system based on adaptive control. The major components of the biogas fuel power system are modeled in detail. Initially estimated the volume of methane gas produced by the biogas reactor. Modeled microturbine with adaptive control in the second stage. The mechanical parameters such as load torque and speed are obtained. The rectified output from the microturbine is used to power the permanent magnet synchronous generator and the permanent magnet synchronous motor, respectively. It is observed that the system responds with respect to variations in the load. The electrical parameters such as frequency of generated voltage, output voltage, output current, and generated DC voltage across DC motor are obtained. Also studied the relation of methane gas output to the retention period. The experimental findings show that the retention time varies between 25 and 45 days. The results say that parameters are within the tolerance band, and the model works correctly. Hence the biogas fuel power system with the adaptive control system is suitable for rural electrification purposes such as DC water pumping applications especially in rural area.

ACKNOWLEDGEMENTS

We acknowledge to Visvesvaraya Technological University, Belgaum, Karnataka, India for support in completing this research work successfully.




REFERENCES

- [1] M. Saeed, S. Fawzy, and M. El-Saadawi, "Modeling and simulation of biogas-fueled power system," *International Journal of Green Energy*, vol. 16, no. 2, pp. 125–151, Jan. 2019, doi: 10.1080/15435075.2018.1549997.
- [2] K. Pathmasiri, F. A. Haugen, and S. Gunawardena, "Simulation of a biogas reactor for dairy manure," in *Annual Transactions of IESL. The Institution of Engineers, Sri Lanka*, 2013, pp. 394–398.
- [3] S. Fawzy, M. Saeed, A. Eladl, and M. El-Saadawi, "Adaptive control system for biogas power plant using model predictive control," *Journal of Modern Power Systems and Clean Energy*, vol. 9, no. 5, pp. 1193–1204, 2021, doi: 10.35833/MPCE.2019.000170.
- [4] A. Kasinath *et al.*, "Biomass in biogas production: pretreatment and codigestion," *Renewable and Sustainable Energy Reviews*, vol. 150, p. 111509, Oct. 2021, doi: 10.1016/j.rser.2021.111509.
- [5] C. A. Hampel and R. J. Braun, "Off-design modeling of a microturbine combined heat and power system," *Applied Thermal Engineering*, vol. 202, p. 117670, Feb. 2022, doi: 10.1016/j.applthermaleng.2021.117670.
- [6] S. Achinas, V. Achinas, and G. J. W. Euverink, "A technological overview of biogas production from biowaste," *Engineering*, vol. 3, no. 3, pp. 299–307, Jun. 2017, doi: 10.1016/J.ENG.2017.03.002.
- [7] H. W. Kim, S. S. Kim, and H. S. Ko, "Modeling and control of PMSG-based variable-speed wind turbine," *Electric Power Systems Research*, vol. 80, no. 1, pp. 46–52, Jan. 2010, doi: 10.1016/j.epsr.2009.08.003.
- [8] C. Rieke, D. Stollenwerk, M. Dahmen, and M. Pieper, "Modeling and optimization of a biogas plant for a demand-driven energy supply," *Energy*, vol. 145, pp. 657–664, Feb. 2018, doi: 10.1016/j.energy.2017.12.073.
- [9] G. Oppong, G. A. Montague, and E. B. Martin, "Towards model predictive control on anaerobic digestion process," *IFAC Proceedings Volumes (IFAC-PapersOnline)*, vol. 10, no. PART 1, pp. 684–689, Dec. 2013, doi: 10.3182/20131218-3-IN-2045.00063.
- [10] H. Parveen, U. Sharma, and B. Singh, "Battery supported solar water pumping system with adaptive feed-forward current estimation," *IEEE Transactions on Energy Conversion*, vol. 37, no. 3, pp. 1623–1633, Sep. 2022, doi: 10.1109/TEC.2022.3147496.
- [11] A. Derizadeh, O. Karabasoglu, M. P. Calasan, and F. Mehdipour, "A dynamic functional model of diode bridge rectifier for unbalanced input voltage conditions," *IET Power Electronics*, vol. 14, no. 3, pp. 584–589, Feb. 2021, doi: 10.1049/pe12.12040.




- [12] V. Sankardoss and P. Geethanjali, "Parameter estimation and speed control of a PMDC motor used in wheelchair," *Energy Procedia*, vol. 117, pp. 345–352, Jun. 2017, doi: 10.1016/j.egypro.2017.05.142.
- [13] X. Xu, K. Li, F. Qi, H. Jia, and J. Deng, "Identification of microturbine model for long-term dynamic analysis of distribution networks," *Applied Energy*, vol. 192, pp. 305–314, Apr. 2017, doi: 10.1016/j.apenergy.2016.08.149.
- [14] Q. Zhang, J. He, Y. Xu, Z. Hong, Y. Chen, and K. Strunz, "Average-value modeling of direct-driven PMSG-based wind energy conversion systems," *IEEE Transactions on Energy Conversion*, vol. 37, no. 1, pp. 264–273, Mar. 2022, doi: 10.1109/TEC.2021.3095486.
- [15] H. Nikkhajoei and R. Iravani, "Electromagnetic transients of a micro-turbine based distributed generation system," *Electric Power Systems Research*, vol. 77, no. 11, pp. 1475–1482, Sep. 2007, doi: 10.1016/j.epsr.2006.08.019.
- [16] W. Ahmed and J. Rodríguez, "A model predictive optimal control system for the practical automatic start-up of anaerobic digesters," *Water Research*, vol. 174, p. 115599, May 2020, doi: 10.1016/j.watres.2020.115599.
- [17] A. Y. Fershalov, Y. Y. Fershalov, and M. Y. Fershalov, "Principles of designing gas microturbine stages," *Energy*, vol. 218, p. 119488, Mar. 2021, doi: 10.1016/j.energy.2020.119488.
- [18] R. I. Putri, M. Pujiantara, A. Priyadi, T. Ise, and M. H. Purnomo, "Maximum power extraction improvement using sensorless controller based on adaptive perturb and observe algorithm for PMSG wind turbine application," *IET Electric Power Applications*, vol. 12, no. 4, pp. 455–462, Apr. 2018, doi: 10.1049/iet-epa.2017.0603.
- [19] T. Nevzorova and V. Kutcherov, "Barriers to the wider implementation of biogas as a source of energy: a state-of-the-art review," *Energy Strategy Reviews*, vol. 26, p. 100414, Nov. 2019, doi: 10.1016/j.esr.2019.100414.
- [20] H. M. Usman, S. Mukhopadhyay, and H. Rehman, "Permanent magnet DC motor parameters estimation via universal adaptive stabilization," *Control Engineering Practice*, vol. 90, pp. 50–62, Sep. 2019, doi: 10.1016/j.conengprac.2019.06.006.
- [21] N. V. Kuznetsov, G. A. Leonov, S. M. Seledzhi, M. V. Yuldashev, and R. V. Yuldashev, "Nonlinear analysis of phase-locked loop with squarer," *IFAC Proceedings Volumes (IFAC-PapersOnline)*, vol. 46, no. 12 PART 1, pp. 80–85, 2013, doi: 10.3182/20130703-3-FR-4039.00027.
- [22] P. Gupta, C. Kurien, and M. Mittal, "Biogas (a promising bioenergy source): a critical review on the potential of biogas as a sustainable energy source for gaseous fuelled spark ignition engines," *International Journal of Hydrogen Energy*, vol. 48, no. 21, pp. 7747–7769, Mar. 2023, doi: 10.1016/j.ijhydene.2022.11.195.
- [23] D. Liu *et al.*, "Exploring biomass power generation's development under encouraged policies in China," *Journal of Cleaner Production*, vol. 258, p. 120786, Jun. 2020, doi: 10.1016/j.jclepro.2020.120786.
- [24] C. Xu, J. Hong, J. Chen, X. Han, C. Lin, and X. Li, "Is biomass energy really clean? An environmental life-cycle perspective on biomass-based electricity generation in China," *Journal of Cleaner Production*, vol. 133, pp. 767–776, Oct. 2016, doi: 10.1016/j.jclepro.2016.05.181.
- [25] J. A. Ruiz, M. C. Juárez, M. P. Morales, P. Muñoz, and M. A. Mendivil, "Biomass gasification for electricity generation: review of current technology barriers," *Renewable and Sustainable Energy Reviews*, vol. 18, pp. 174–183, Feb. 2013, doi: 10.1016/j.rser.2012.10.021.

BIOGRAPHIES OF AUTHORS



Vineeth Kumar Pothera Kariyat    is currently working as an assistant professor in the department of electronics and communication engineering at Sri Venkateshwara College of Engineering, Bengaluru, Visvesvaraya Technological University, India. He received B. Tech degree in electrical and electronics engineering from Kannur University, Kerala in 2011. He received M.Tech. degree in power and energy from Amrita Vishwavidyapeetham University, Coimbatore, Tamil Nadu, India. His area of interest includes power electronics and renewable energy resources. To his credit prolifically published eight papers in international conferences and three reputed international journals. He can be contacted at email: vineethkumarpk@gmail.com.



Dr. Jijesh Jisha Janardhanan    is currently working as Professor and HoD in the Electronics and Communication Department at Sri Venkateshwara College of Engineering, Visvesvaraya Technological University, Bangalore. He received the B. Tech. degree in Electronics and Communication Engineering from Kannur University in 2006, and earned M. Tech. degree in Electronics from Visvesvaraya Technological University, Belguam, in 2010 and awarded doctorate degree in the field of wireless communication from Visvesvaraya Technological University, Belguam, in 2018-2019. He has more than 53 publications in his credit in various prestigious journals. His area of interest includes wireless communication, VLSI, and renewable energy sources. He can be contacted at email: jijeshjj4u@gmail.com.